

High Resolution Radar Target Modeling Using a Modified Prony Estimator

Rob Carrière, *Student Member, IEEE*, and Randolph L. Moses, *Senior Member, IEEE*

Abstract—A method for characterizing radar signatures using a Prony model is developed based on the concept of scattering centers. A parameterization of the Prony model specific to the radar target identification problem is chosen, and several key improvements to the algorithm, including the use of singular value decomposition and the removal of spurious scattering centers are presented. The resulting algorithm is tested with data taken from a compact range. These tests include comparison of different targets, different aspect angles and frequency ranges, as well as robustness tests on the algorithm and evaluation of performance in noise.

I. INTRODUCTION

A large amount of work has been done on numerical approximations of the inverse scattering problem, both for fundamental electromagnetic purposes and for diverse applications [1]–[8]. For high frequency data, many objects are well approximated as a set of discrete scattering centers, so the inverse scattering problem may be approximated by a scattering center extraction problem. Thus, one approach to inverse scattering is to estimate a time-domain scattering profile of the object, and to locate scattering centers from peaks in the time-domain profile.

One commonly used method is to perform an inverse discrete Fourier transform (IDFT) operation on frequency-domain scattering measurements to obtain the time (or range) domain profile. The scattering centers are then found from peaks in this profile. In this approach, a set of N frequency measurements is converted into an N -point range profile. By use of zero padding, the range profile can be interpolated to obtain more than N points on a finer grid. In either case, one ends up with a set of sample points which nonparametrically describe the range profile.

In this paper we seek to locate and characterize the discrete scattering centers of an object by using a parametric scattering model, specifically the Prony model. This paper shows that the Prony method can be used to obtain robust, high resolution scattering information on realistic radar targets.

In this paper we consider the use of the Prony model for high resolution modeling of complex targets. Our work is aimed at employing the Prony model estimates for automatic

target recognition (ATR) systems. There are two reasons that the Prony model is attractive. First, the Prony method is not inherently resolution-limited as is the IDFT. As a result, the Prony-based algorithm is able to resolve scattering centers that are separated by less than the IDFT resolution limit. Furthermore, the Prony method directly provides the ranges of the scatterers, eliminating the need for peak-finding algorithms or other methods of locating scatterers from an IDFT range profile.

The Prony model was considered in [5], where it was shown that the model is exact for point scatterers. For diffraction scattering terms, there is a mismatch between the Prony model and the physical scattering process. However, it is shown in [5] that this mismatch does not significantly degrade the accuracy of the estimates even for fairly large relative bandwidths. This paper can be considered an extension of [5], where we consider complex targets and investigate estimation algorithm issues which improve modeling accuracy for complex targets.

The standard Prony algorithm is a well-established signal processing procedure [9], [10]. However, it suffers from several shortcomings when applied to radar data. First, for most targets there will be more scattering terms present than can be modeled; this can affect the performance of the algorithm. Second, the Prony method can be sensitive to noise, as has been documented in the signal processing literature [10]. Third, the Prony method requires an *a priori* selection of the model order. Since the model parameter estimates are also sensitive to the choice of this order, it is important to select the order “correctly” for a given data set. One of the main contributions of this paper is the development of an estimation algorithm which improves the performance of the Prony method for radar scattering data.

An outline of this paper is as follows. In Section II we discuss the use of the Prony algorithm in the inverse scattering problem. In Section III we describe the modified Prony algorithm, and in Section IV we present experimental results obtained by applying the modified Prony algorithm to data taken with the compact range at the ElectroScience Laboratory of the Ohio State University (OSU). The targets are models of commercial aircraft. Section V concludes the paper.

II. USE OF THE PRONY METHOD IN THE INVERSE SCATTERING PROBLEM

Assume that we have available N relatively coherent radar cross section (RCS) measurements of a target at equally

Manuscript received June 7, 1990; revised July 15, 1991. This work was supported in part by the Office of Naval Research under Contract N00014-87-K-2011.

The authors are with the ElectroScience Laboratory, Department of Electrical Engineering, The Ohio State University, Columbus, OH 43210. IEEE Log Number 9105267.

spaced frequency steps. Denote these (complex-valued) measurements as $\{y_k\}_{k=0}^{N-1}$ taken at frequencies

$$f_k = f_0 + k\delta_f, \quad k = 0 \cdots N-1. \quad (1)$$

The approach we take is to model the RCS measurements as a sum of damped complex exponential sequences:

$$y_k = \sum_{i=1}^m d_i p_i^k, \quad k = 0 \cdots N-1. \quad (2)$$

In (2) m is the model order and has to be preselected. The parameters $\{d_i\}_{i=1}^m$ and $\{p_i\}_{i=1}^m$ are parameters to be estimated; they will be referred to as the *amplitudes* and the *zeros* of the model, respectively. We will refer to (2) as the Prony model for the RCS data.

Geometrically relevant information can be retrieved from the estimated values of the $\{d_i\}_{i=1}^m$ and $\{p_i\}_{i=1}^m$ parameters as is shown by taking the inverse Fourier transform (IFT) of (2)¹:

$$Y(r) = \sum_{i=1}^m \frac{d_i e^{j\pi(1-2r/R)}}{e^{j\pi(1-2r/R)} - p_i}, \quad 0 \leq r \leq R \quad (3)$$

(where $r = ct$). We have used the relative range r as the independent variable instead of time, because range relates more directly to the target geometry. The constant R is the maximum unambiguous range given by $R = c/2\delta_f$.

From (3) we can see that the contribution of the i th component of the Prony model will produce a peak at a range r_i given approximately by the argument of p_i :

$$r_i \approx \left(\frac{1}{2} - \frac{\arg p_i}{2\pi} \right) R. \quad (4)$$

That is, the i th component describes a scattering center at relative range r_i . We can obtain further information about this scattering center by observing that the sharpness of the peak at r_i is dictated by the modulus of p_i . Defining $\rho_i = |p_i|$, we see that if $\rho_i \approx 1$, the denominator of the i th term in (3) will be nearly zero for $r \approx r_i$, causing large changes in the contribution of the term to $Y(r)$. This means we obtain a sharp, narrow peak at range r_i . Values of ρ_i not near one lead to a broader peak. $\rho_i < 1$ corresponds to a tip diffraction, and $\rho_i > 1$ corresponds to specular scattering from plates and dihedrals [5], [11]. Thus, ρ_i describes the degree to which the i th scattering center is concentrated in range.

Finally, the energy of each scattering center can be computed from the contribution of the scattering center's component of RCS data. Each component is given by $\{d_i p_i^k\}_{k=0}^{N-1}$ (see (2)). The energy P_i of this component is

$$P_i = \sum_{k=0}^{N-1} |d_i p_i^k|^2 = |d_i|^2 \frac{1 - \rho_i^{2N}}{1 - \rho_i^2}. \quad (5)$$

To summarize, the Prony model provides a downrange re-

¹ Equation (3) is obtained under the assumption that the sampled frequency response in (2) is extrapolated for $-\infty < k < \infty$; a more realistic assumption would be that the frequency response can be extrapolated only for a finite amount $K_1 < k < K_2$. In the latter case, the range response is given by $Y(r)$ in (3) convolved by a sinc function whose width is proportional to $1/(K_2 - K_1)$.

sponse profile of the target predetermined by m scattering centers at ranges r_i . Each of these scattering centers is characterized by the corresponding amplitude d_i and zero p_i parameters. These $2m$ parameters $\{d_i, p_i\}_{i=1}^m$ characterize the target scattering and could be used as a feature vector for a target recognition system.

III. THE MODIFIED PRONY ALGORITHM

This section describes a method for estimating the parameters $\{d_i, p_i\}_{i=1}^m$ from stepped-frequency measurements. Central to the algorithm is the use total least squares coupled with singular value decomposition (SVD). Singular value decomposition is helpful in increasing the accuracy of the parameter estimates [12]–[14]. In addition, with the use of SVD one can set an upper bound M on the model order; an automatic method of choosing the Prony model order $m < M$ is discussed. The combined use of a high prediction order M and a data-driven selection of m provides for improved robustness of the algorithm with respect to noise and to target aspect changes (see also [15]). A related application is discussed in [16], in which Prony's method coupled with SVD is used to estimate complex natural resonances from time-domain radar backscatter responses.

We now consider how to estimate the parameters $\{d_i\}_{i=1}^m$ and $\{p_i\}_{i=1}^m$ from the data $\{y_k\}_{k=0}^{N-1}$. We use the total least squares prony method [13], coupled with singular value decomposition. We estimate $\{p_i\}_{i=1}^m$ by introducing a monic polynomial $A_M(z) = z^M + a_1 z^{M-1} + \cdots + a_M$ of order $M \geq m$ that has zeros $\{p_i\}_{i=1}^M$. Of these M zeros, m zeros correspond to scattering centers in the Prony model in (2), and the remaining zeros are spurious "computation" zeros. We estimate the coefficients $\{a_i\}_{i=1}^M$ by constructing a system of backward linear prediction equations that expresses the coefficients of $A_M(z)$ in terms of the RCS data $\{y_k\}_{k=0}^{N-1}$. In matrix form we obtain [10]

$$\begin{bmatrix} y_{M+1} & y_M & \cdots & y_1 \\ y_{M+2} & y_{M+1} & \cdots & y_2 \\ \vdots & \vdots & \ddots & \vdots \\ y_{N-1} & y_{N-2} & \cdots & y_{N-M-1} \end{bmatrix} \begin{bmatrix} a_M \\ \vdots \\ a_1 \\ 1 \end{bmatrix} \approx 0$$

or

$$Y \hat{A}_M \approx 0. \quad (6)$$

To solve for the linear prediction coefficients, we use total least squares with SVD. We first form the SVD of Y ,

$$Y = U \Sigma V^H \quad (7)$$

where U and V are unitary matrices, and Σ is a diagonal matrix, given by

$$\Sigma = \begin{bmatrix} \sigma_1 & & & & & \\ & \sigma_2 & & & & \\ & & \ddots & & & \\ & & & \sigma_j & & \\ \mathbf{0} & & & & & \end{bmatrix}_{(N-M-1) \times (M+1)}, \quad \sigma_1 \geq \sigma_2 \geq \cdots \geq \sigma_j \geq 0 \quad (8)$$

(where $J = \min(M + 1, N - M - 1)$). If the RCS measurements are noiseless and correspond exactly to the model in (2), then Y has rank m and only the first m singular values in (8) are nonzero. In practice this is not the case. To reduce some of the effects of noise and modeling error, Σ is replaced by

$$\Sigma' = \begin{bmatrix} \sigma_1 & & & & \mathbf{0} \\ & \ddots & & & \\ & & \sigma_m & & \\ \mathbf{0} & & & & 0 \end{bmatrix}_{(N-M-1) \times (M+1)} \quad (9)$$

In practice the correct model order m is not known *a priori*, so must be estimated. We obtain an estimate of m from the singular values $\{\sigma_i\}_{i=1}^J$ as follows: if the scattering data fit the model exactly and there was no noise, $\sigma_{m+1} = \sigma_{m+2} = \dots = \sigma_J = 0$. In the presence of noise and model mismatch the matrix Y will have full rank, but will be "close" to a matrix Y' of rank m and we have $\sigma_{m+1} \approx \sigma_{m+2} \approx \dots \approx \sigma_J \approx 0$. The value of m to be used can be fixed or we can find a data adaptive value from the estimated singular values. Simple adaptive tests include choosing m such that σ_{m+1} is the first singular value smaller than $s\sigma_1$, with $0 < s < 1$ fixed, or choosing m as the smallest number such that $\sigma_{m+1} - \sigma_m < s(\sigma_1 - \sigma_2)$. More complex tests can be found from information-theoretic considerations, see [17] and [18].

The vector \hat{A}_M is found by solving

$$U\Sigma'V^H\hat{A}_M = 0 \quad (10)$$

in the total least squares sense [13]. Next, the zeros $\{\hat{p}_i\}_{i=1}^M$ of $\hat{A}_M(z)$ are obtained by polynomial root finding techniques. Of these M zeros, m are the desired zeros.

The estimates \hat{d}_i are found as the ordinary least squares solution of (2) given the zero estimates $\{\hat{p}_i\}_{i=1}^M$. Thus,

$$\begin{bmatrix} \hat{d}_1 \\ \vdots \\ \hat{d}_M \end{bmatrix} = (\hat{P}^H\hat{P})^{-1}\hat{P}^Hy \quad (11)$$

where

$$\hat{P} = \begin{bmatrix} \hat{p}_1^0 & \dots & \hat{p}_M^0 \\ \vdots & & \vdots \\ \hat{p}_1^{N-1} & \dots & \hat{p}_M^{N-1} \end{bmatrix} \quad y = \begin{bmatrix} y_0 \\ \vdots \\ y_{N-1} \end{bmatrix}$$

Now the m scattering zeros must be separated from the computation zeros. The method we use is to compute the energy P_i in (5) of each estimated zero-amplitude pair $\{\hat{p}_i, \hat{d}_i\}$, for $i = 1, \dots, M$. Only the m modes with the highest energies are kept. This procedure has the advantage of robustness: the highest energy components are selected, and these are expected to suffer the least degradation as a result of noise and clutter in the data. In this way, the algorithm automatically selects the final model order, which is adequate to model the particular data set.

Once the mode selection process has been completed, the target scattering is represented by the m pairs $\{\hat{p}_i, \hat{d}_i\}_{i=1}^m$.

These pairs form the feature vector for the target.² Alternately, the corresponding downrange response profile can be found by substituting these quantities into (3).

IV. EXPERIMENTAL RESULTS

In this section we present the results of applying the above algorithm to data measured at the ElectroScience Laboratory Compact Range Facility. The stepped-frequency measurements consist of amplitude and phase of the radar return from the target at each frequency. The radar receiver in the OSU compact range uses a time gate to eliminate spurious scattering effects from the anechoic chamber. The data are then calibrated by subtracting the response of the empty chamber and dividing by the calibrated response of a reference target. Details of the measurement system and calibration procedure are described in [19]. In all cases the transmit and the receive polarizations are horizontal. White Gaussian noise is then added to these measurements to simulate noisy measurements.

For the experiments presented below, the RCS data measurements were taken from scale models of commercial aircraft. For each model, we list the equivalent the frequency range for the full-scale target. We show a properly scaled drawing of the target and the range profile using the inverse DFT of the RCS data (with a Hanning window and zero-padding to 512 points.)

Fig. 1 shows the estimated downrange response of a Boeing 707. We used $N = 31$ scattering measurements of the scaled target from 18–26.5 GHz; this corresponds to measurements taken at 120–176 MHz on the full-size aircraft. We used a model order $M = 15$ and reduced to both $m = 5$ and $m = 10$ singular values. Also shown is the range profile obtained using a (zero-padded) IDFT of the 31 data points. For $m = 5$, we see three prominent peaks which correspond to the engine inlets and wing structure. When m is increased to 10, we see the three main peaks are retained (although with somewhat different amplitudes), but additional detail now becomes visible. The small peak on the left in Fig. 1 corresponds to the nose of the aircraft, the peak at 46 m corresponds to the wing tips, and the two peaks at 59 and 62 m correspond to the tail and to a target postresonance. Thus, for low model orders the major scattering behavior is estimated, and the finer details of the scattering behavior are estimated as the model order is increased.

Comparison of the Prony profiles to the IDFT profile in Fig. 1 shows that the two are in good overall agreement. Note in particular that the Prony algorithm resolved the two pairs of engine inlets, whereas the IDFT method did not.

Fig. 2 shows the response of a Boeing 707 at an aspect angle of 15° , with $M = 15$ and $m = 10$. At this angle the response of the inner left and the outer right engine inlet occur at almost the same downrange point. Similarly the inner right engine inlet and the joint of the left wing are very close in range. In the figure we observe a set of four large responses in the center that model the two combined struc-

² The mode amplitudes can be updated by solving (11) using only the m selected zeros; we have found that this updating has little effect on the overall estimates, however.

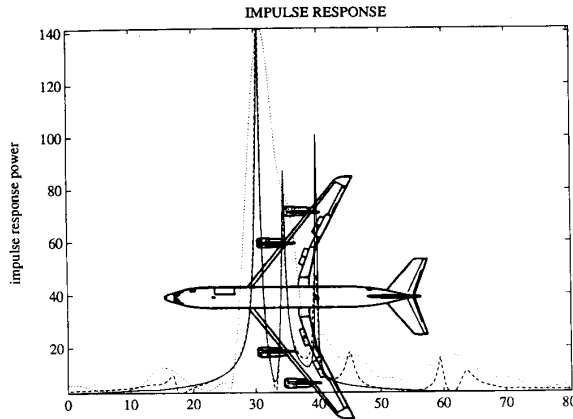


Fig. 1. Downrange response of the Boeing 707 using $N = 31$ data points from 120–176 MHz, model order $M = 15$, using $m = 5$ (solid line) and $m = 10$ (dashed line) singular values. An IDFT with a Hanning window and zero-padded to 512 points is also shown (dotted line).

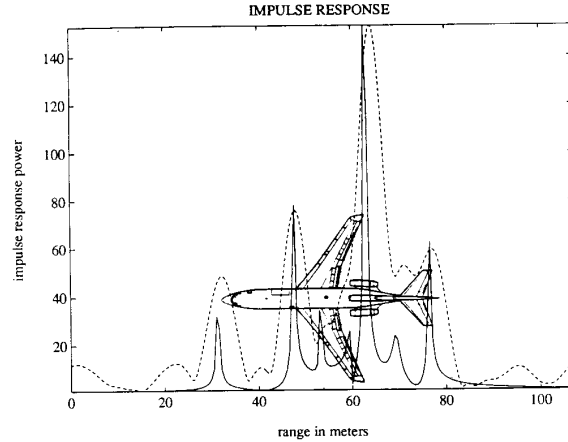


Fig. 3. Downrange response of the Boeing 727 using $N = 31$ data points from 90–133 MHz. Solid line: Prony model with $M = 15$ and $m = 10$. Dotted line: IDFT of the data using a Hanning window.

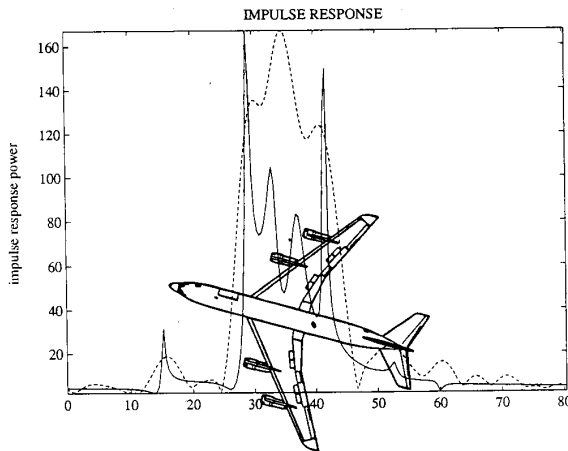


Fig. 2. Downrange response of the Boeing 707 at an aspect angle of 15° using $N = 31$ data points from 120–176 MHz. Solid line: Prony model with $M = 15$ and $m = 10$. Dotted line: IDFT of the data using a Hanning window.

tures mentioned above as well as the wingtips. The tail response is also modeled at the expected location. This experiment shows that the response varies in a predictable way with the aspect angle.

Fig. 3 shows the response of the Boeing 727 also taken with $N = 31$ data points from 18–26.5 GHz (this corresponds to 90–133 MHz for a full-size aircraft). We used model order $M = 15$ and kept $m = 10$ singular values and zeros. The small peak at 52 m is attributed to the support pedestal. Note the resolution of wingtips and engine inlets by the Prony method, and the better localization of scattering mechanisms when compared to the IDFT.

Fig. 4 shows the results for the Boeing 707 as in Fig. 1, but with white Gaussian noise added at a signal-to-noise ratio (SNR) of 10 dB. Here, SNR is the ratio of signal energy and noise energy: $\text{SNR} = \sum_{k=0}^{N-1} |y_k|^2 / \sum_{k=0}^{N-1} |n_k|^2$. We used $M = 15$ and both $m = 10$ and $m = 5$. For each value of m we show 10 overlapped estimates from 10 independent noise

realizations. We observe that the reduction of the number of singular values eliminates most of the noise peaks, while retaining the signal peaks. For the $m = 5$ case we also observe that the location of the peaks is estimated reliably despite the noise. The amplitudes show more variation, but are still quite consistent for the two major peaks. Notice that the response at 63 m in Fig. 4 for $m = 5$ appears in the noiseless scattering response for $m = 10$, so it does correspond to target geometry. The peak at 7 m is a spurious peak from one of the noise realizations; its energy is 19 dB below the energy of the main peak.

In the context of automatic target recognition, the Prony model parameters can be used as features for target classification. To this end, several points are worth mentioning. First, the Prony method offers the potential of resolution enhancement; the scattering centers are often highly localized, and as was seen in Fig. 1, the Prony method is capable of resolving scattering centers which cannot be resolved by using IDFT. In addition, the Prony method represents the scattering by a geometrically relevant parameter vector which is generally of lower dimension than the original data vector. In the examples considered, the original data consists of 31 complex numbers, whereas the Prony model consists of $2m$ complex parameters. This results in 68% data reduction for $m = 5$ and a 35% reduction for $m = 10$. These data reduction percentages are conservative because: 1) zero padding is often employed to improve the range resolution by a factor of 3–4 in IDFT range profiles, and 2) the phase angle of d_i does not seem to be useful for target recognition and could probably be discarded. Finally, we remark that many IDFT-based ATR methods employ some sort of peak extraction from the range profile; if the Prony method is used this peak extraction step is unnecessary.

V. CONCLUSION

We have considered a Prony model for the estimation of radar target scattering centers from frequency domain data. We employed an SVD-based algorithm that is robust with

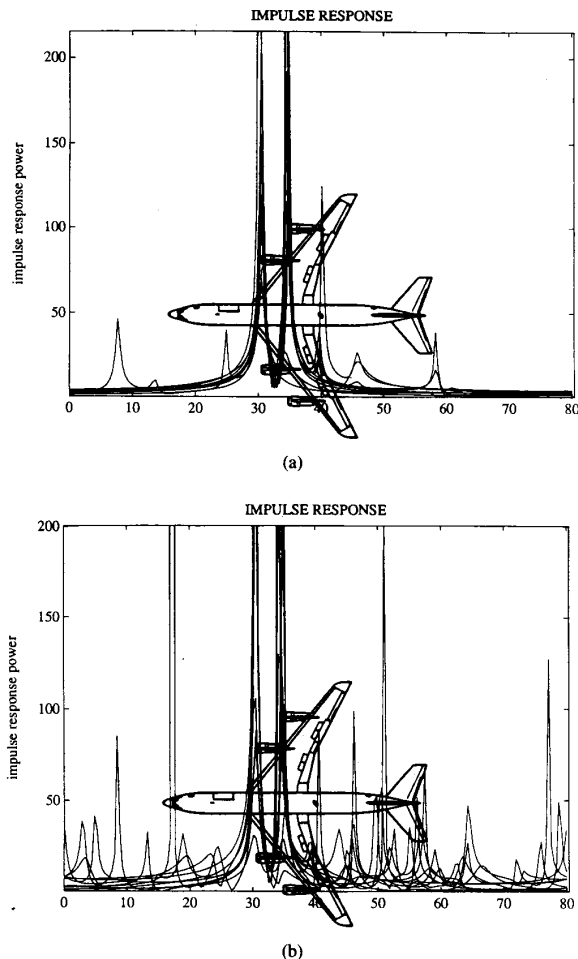


Fig. 4. Ten overlaid noisy downrange responses of the Boeing 707 at 0° , using $N = 31$ data points from 120–176 MHz, model order $M = 15$ and $\text{SNR} = 10$ dB. (a) $m = 5$. (b) $m = 10$.

respect to changes in the model parameters and to changes in the frequency band employed. We have also shown that the algorithm performs reliably in the presence of noise. Using compact range scattering data, we have shown that different targets do indeed produce different response estimates, and that varying the aspect angle of the target by 15° leads to smooth and predictable changes in the estimated response for data in this frequency range.

The algorithm requires the user to choose an upper bound M on the model order: the final order m is selected automatically. The algorithm can thus be used to estimate feature vectors for an automatic target recognition system. The estimated model parameters would be features supplied to a classification stage in an ATR system. This method has the advantage that the signal processing stage can serve to both transform the frequency data into geometrically relevant information and perform data compression (the number of parameters output by the algorithm is less than the number of data points). This is important for the computational burden imposed by the classifier stage. The performance of such a

two stage classification procedure is currently being investigated.

REFERENCES

- [1] T. K. Sarkar, D. D. Weiner, and V. K. Jain, "Some mathematical considerations in dealing with the inverse problem," *IEEE Trans. Antennas Propagat.*, vol. AP-19, pp. 373–379, Mar. 1981.
- [2] W.-M. Boerner, M. B. El-Arini, C.-Y. Chan, and P. M. Mastoris, "Polarization dependence in electromagnetic inverse problems," *IEEE Trans. Antennas Propagat.*, vol. AP-29, pp. 262–270, Mar. 1981.
- [3] Y. Das and W.-M. Boerner, "On radar target shape estimation using algorithms for reconstruction from projections," *IEEE Trans. Antennas Propagat.*, vol. AP-26, pp. 274–279, Mar. 1978.
- [4] L. W. Pearson and D. R. Roberson, "The extraction of the singularity expansion description of a scatterer from sampled transient surface current response," *IEEE Trans. Antennas Propagat.*, vol. AP-28, pp. 182–190, Mar. 1980.
- [5] M. P. Hurst and R. Mittra, "Scattering center analysis via Prony's method," *IEEE Trans. Antennas Propagat.*, vol. AP-35, pp. 986–988, Aug. 1987.
- [6] R. Weyker and D. Dudley, "Asymptotic model-based identification of an acoustically rigid sphere," *Wave Motion*, vol. 9, no. 9, pp. 77–97, 1987.
- [7] D. G. Dudley, "A state-space formulation of transient electromag-

- netic scattering," *IEEE Trans. Antennas Propagat.*, vol. AP-33, pp. 1127-1130, Oct. 1985.
- [8] M. L. van Blaricum and R. Mittra, "A technique for extracting the poles and residues of a system directly from its transient response," *IEEE Trans. Antennas Propagat.*, vol. AP-23, pp. 777-781, Nov. 1975.
- [9] F. B. Hildebrand, *Introduction to Numerical Analysis*. New York: McGraw-Hill, 1974.
- [10] L. Marple, *Digital Spectral Analysis with Applications*. Englewood Cliffs, NJ: Prentice-Hall, 1987.
- [11] W. Leeper, "Identification of scattering mechanisms from measured impulse response signatures of several conducting objects," Master's thesis, Ohio State Univ., Columbus, OH, 1984.
- [12] R. Kumaresan and D. W. Tufts, "Estimating the parameters of exponentially damped sinusoids and pole-zero modeling in noise," *IEEE Trans. Acoust., Speech, Signal Processing*, vol. ASSP-30, pp. 833-840, Dec. 1982.
- [13] M. A. Rahman and K.-B. Yu, "Total least squares approach for frequency estimation using linear prediction," *IEEE Trans. Acoust., Speech, Signal Processing*, vol. ASSP-35, pp. 1440-1454, Oct. 1987.
- [14] R. Moses, J. Li, and P. Stoica, "Accuracy properties of high order Yule-Walker equation estimators of sinusoidal frequencies," in *8th IFAC Symp. Identification and Syst. Parameter Estimation*, Aug. 27-31, 1988.
- [15] R. Carrière and R. L. Moses, "High resolution radar target modeling using ARMA models," Dept. Elect. Eng., Ohio State Univ., ElectroSci. Lab., Columbus, OH, Tech. Rep., May 1989.
- [16] J. Auton and M. van Blaricum, "Investigation of resonance extraction from noisy transient electromagnetics data," General Res. Corp., Tech. Rep. CR-81-984, Aug. 1981.
- [17] M. Wax and T. Kailath, "Detection of signals by information theoretic criteria," *IEEE Trans. Acoust., Speech, Signal Processing*, vol. ASSP-33, pp. 387-392, Apr. 1985.
- [18] M. Wax and I. Ziskind, "Detection of the number of coherent signals by the MDL principle," *IEEE Trans. Acoust., Speech, Signal Processing*, vol. 37, pp. 1190-1196, Aug. 1989.
- [19] A. Kamis, E. K. Walton, and F. D. Garber, "Radar target identification techniques applied to a polarization diverse aircraft data base," ElectroSci Lab., Dept. Elec. Eng., Ohio State Univ., Columbus, OH, Tech. Rep. 717220-2, Mar. 1987.



Rob Carrière (S'86) was born on November 13, 1961. He received the M.S. (ingenieur) degree in electrical engineering from the Eindhoven University of Technology, Eindhoven, The Netherlands, in 1987. He is currently pursuing the Ph.D. degree in electrical engineering at The Ohio State University, Columbus.

His current research interests are in digital signal processing and include parametric time series analysis and radar signal processing.



Randolph L. Moses (S'78-M'85-SM'90) received the B.S., M.S., and Ph.D. degrees in electrical engineering from Virginia Polytechnic Institute and State University, Blacksburg, in 1979, 1980, and 1984, respectively.

During the summer of 1983 he was a SCEEE Summer Faculty Research Fellow at the Rome Air Development Center, Rome, NY. From 1984 to 1985 he was with the Eindhoven University of Technology, Eindhoven, The Netherlands, as a NATO Postdoctoral Fellow. Since 1985 he has

been with the Department of Electrical Engineering, The Ohio State University, Columbus, where he is currently an Associate Professor. His research interests are in digital signal processing, and include parametric time series analysis, radar signal processing, system identification, and model reduction.

Dr. Moses is a member of Eta Kappa Nu, Tau Beta Pi, Phi Kappa Phi, and Sigma Xi.